Remote optical turbulence sensing: present and future

Andrei Tokovinin *
Cerro Tololo Inter-American Observatory, La Serena, Chile

December 20, 2007

1 General perspective

Refractive index of atmospheric air is non-homogeneous and distorts propagating light waves. This phenomenon, called *optical turbulence*, causes serious limitations in astronomy, optical communication, adaptive optics, etc., driving the need for turbulence characterization. At the same time, these distortions provide means to measure the optical turbulence by a *remote optical turbulence sensor* (ROTS). Compared to direct *in situ* techniques such as micro-thermal probes, a ROTS has obvious advantages: it can sample the whole turbulent path instantaneously and measures the *optical* effect, directly related to the propagation, hence to the needs of the end users. Unfortunately, the information on turbulence delivered by existing ROTSs is always incomplete due to the limitations of these techniques.

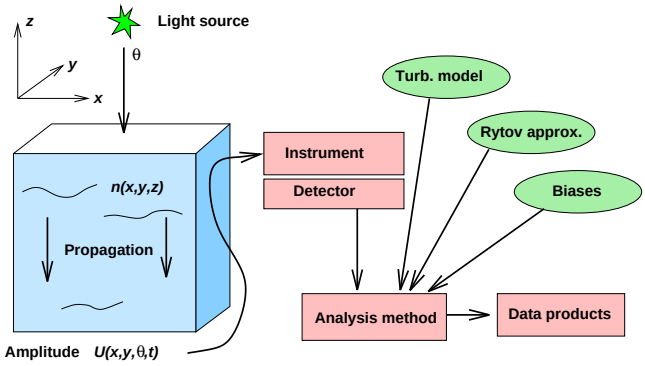

Figure 1: Remote optical turbulence sensing

Figure 1 gives an overview of a general ROTS and its major components, discussed below one by one.

* *Corresponding author address:* Andrei Tokovinin, Cerro Tololo Inter-American Observatory, Casilla 603, La Serena, Chile
E-mail: atokovinin@ctio.noao.edu

The light source must be located outside the turbulent volume. Bright stars (one, two, or several) are most convenient ROTS sources available at no cost and distributed over the whole sky. Extended sources (Sun, Moon, or planets) can be used as well. The uniqueness of these solar-system bodies pre-selects the light path (a ROTS can only work when the source is visible) and does not permit to sample the atmosphere when and where we want. In this sense, artificial laser guide stars (LGS) are ideal, being created at will where needed. The cost of an LGS is, however, prohibitively high for turbulence monitoring (primarily because of the high laser power needed to get enough back-scattered photons), so these sources are suitable for a ROTS only when they are created for other purpose such as adaptive optics (AO). On the other hand, low-power laser beams are convenient for turbulence sounding on a horizontal path. In principle, an artificial light source can be placed on a mast, airplane, or satellite to serve for a ROTS. For example, a 30-m solar reflector on a geo-stationary satellite can permanently illuminate one hemisphere, creating a near-stationary bright "star" for ROTS.

Optical turbulence can be mapped as an instantaneous 3D distribution of refractive-index fluctuations $\Delta n(x, y, z, t)$ by means of turbulence tomography, using several stars (e.g. Tokovinin & Viard, 2001). This is needed in AO for wide-field image correction, but would be an over-kill for turbulence characterization (too much information). Instead, a random-process model is assumed. Local turbulence strength is measured by the C_n^2 parameter (*refractive index structure constant*), implying that the refractive-index spatial spectrum obeys the Kolmogorov law between the *turbulence inner scale* l_0 and the *turbulence outer scale* L_0 (Tatarskii, 1961; Roddier, 1981). A frozen-flow assumption permits to describe the temporal evolution of turbulence by the wind speed vector $\mathbf{V}(\mathbf{x})$, where $\mathbf{x} = (x, y, z)$ is a 3D coordinate vector in the turbulent volume.

The random-process model has its obvious limitations. We are dealing with a unique realization of a process which is not stationary in space and time (the turbulence is "patchy", *intermittent*). So, a "local" and/or "instantaneous" $C_n^2(\mathbf{x}, t)$ value implies some spatial and/or temporal averaging and can de defined or measured only approximately. Atmospheric quantities typically vary by several orders of magnitude, so geophysicists are happy to measure them to within a factor of two, in which case the random-process model is adequate. A higher accuracy is sought in optical propagation applications, so, eventually, the limit will be set by the model, rather than by the measurement errors. Until then, the primary *data products* of a ROTS are:

1. *turbulence profile* (TP) $C_n^2(z, t)$ (it is usually assumed that turbulence is stratified horizontally, no dependence on x, y);
2. *wind profile* $\mathbf{V}(z)$ (same assumption), $\mathbf{V} = (V_x, V_y)$
3. *outer scale profile* $L_0(z)$,

and the derivatives of these quantities such as seeing ε_0, isoplanatic angle θ_0, AO time constant τ_0, etc. [See the chapter by J. Vernin]. The inner scale l_0 is almost always irrelevant to optical propagation in astronomy.

Propagation of light through a turbulent volume is such a complex phenomenon that there is no exact theory. Instead, a small-perturbation (Rytov) approximation (Tatarskii, 1961; Roddier, 1981) is universally used to relate turbulence parameters with the light-wave statistics. Depending on the conditions (turbulence intensity, spatial scale, wave-

length), this approximation can be either excellent or poor. Fortunately, modern computing power permits to solve the wave propagation numerically and hence to evaluate or extend the validity of the canonic Rytov theory.

Instrument receives the light waves distorted by the atmosphere and performs some optical transformations. For example, the image of a star or the Sun can be formed at the focus of a small telescope. Alternatively, we can study the distribution of the light amplitude or phase at the pupil plane. The number of potential transformations is unlimited. In the end, the information on the light wave distortion is encoded as a light intensity, and the light is detected by a CCD or some other device.

Analysis method is closely related to the instrument design. The intensity of light in individual detector pixels must be processed, related to the statistics of the wave distortions, and then to the turbulence parameters. Intrinsic limitations or biases, such as photon noise or finite exposure time, must be accounted for. Moreover, the departure of the real instrument from its ideal model can critically affect the results. Suitable methods to discover or monitor instrument parameters and data quality are an essential part of the analysis.

Data products of any given ROTS are either primary quantities (turbulence and wind profiles) or their derivatives such as seeing. Each measurement refers to a particular moment in time and a particular viewing direction. Comparisons between different instruments or between a ROTS and a telescope usually involve different directions, hence are subject to non-stationarity errors.

2 History

The foundations of the propagation theory and turbulence models were set in the 1950s (Chernov, 1960; Tatarskii, 1961). However, quantitative ROTS appeared much later. Good reviews of the basic physics and early techniques are provided by Roddier (1981) and Coulman (1985). Until today, the progress is mainly determined by the available technology. Current explosive development of the ROTSs is just a reflection of our capacity to capture and analyze the light better.

Astronomers took time to assimilate and use the advances of the turbulence theory. First seeing monitors with automatic photo-electric registration of the absolute or differential image motion appeared in the 1960s, and now a Differential Image Motion Monitor (DIMM) is a well-established standard instrument (Sarazin & Roddier, 1990; Tokovinin, 2002b). The idea of DIMM can be traced back to Hosefeld (1954), DIMMs with visual detection were developed by Stock & Keller (1961), a photoelectric DIMM was apparently pioneered by Gillingham (1978). Absolute image motion was first detected photographically with Polar-star trail techniques (Harlan & Walker, 1965), while Babcock (1963) already measured it photo-electrically.

In the 1970s, the Astrophysical Department of the University of Nice led by F. Roddier was at the forefront. Basic ideas of measuring optical turbulence by means of wavefront slopes or scintillation were formulated and tested. The latter method, SCIDAR (SCIntillation Detection And Ranging) (Rocca et al., 1974; Vernin & Azouit, 1983), can deliver turbulence and wind-speed profiles by using a double-star source. It remains one of the most powerful ROTSs until today. The implementation of SCIDAR, now almost trivial, became possible only with an ingenuous real-time image correlator developed by

M. Azouit. It was still a pre-computer era!

Accessibly cheap computers and image detectors appeared finally at the end of 1980s. As both these critical elements improved their performance, so did the ROTSs: DIMMs became faster, SCIDARs cheaper. A Generalized Seeing Monitor (GSM) was the first instrument to measure turbulence outer scale on a routine basis using an old idea of angle-of-arrival correlation (Ziad et al., 2000). Interestingly, GSM employed a now-obsolete image modulation technique (the CCDs were still not fast enough). Yet another step in the ROTS development looks trivial, but turned out to be crucial: the DIMMs became robotic and started to provide a continuous data flow, first at ESO, then at some other observatories. Even today, many ROTS instruments have not passed this milestone and continue to be manually operated, one-time experiments rather than monitors. One of the largest world observatories, Mauna Kea, does not have yet a facility seeing monitor.

The development of ROTS instruments continues in the current decade (2000s) at a fast pace, driven by the increased demand, cheaper components, more computer power, and new ideas.

3 Current techniques

There is an infinite number of ways to derive turbulence characteristics from the statistics of distorted light waves. Which is the best? Where are the limits? Let us try to inter-compare current methods and their potential improvements in trying to answer these questions. The methods are divided in broad classes according to the measurement principle.

3.1 Long exposures

This is a class of methods where the light intensity is averaged over a long time (much longer than the aperture transit time D/V, e.g. for 30 s or more). The effect of turbulence on long exposures is to reduce the effective transverse coherence length of the field to the size of the Fried parameter r_0. The Point Spread Function (PSF) becomes wider, about λ/r_0 rather than diffraction limit λ/D (D – diameter of the aperture, λ – wavelength of light).

The size of point-source (stellar) long-exposure images is a practical and widely used measure of "seeing". The problem of this method is that the PSF is also affected by guiding errors and telescope aberrations, including defocus. We thus deduce from the PSF an upper limit on seeing. At modern telescopes with good optics and guiding, this measure is close to the atmospheric seeing. For example, the best long-exposure images at VLT have FWHM size of $0.2''$, so we may be confident that a FWHM of, say, $0.5''$ is essentially produced by the turbulence. Part of this turbulence can be inside the dome or on the telescope mirror.

The problem of unknown optical aberrations has been avoided elegantly by measuring the fringe contrast in the pupil plane with a *coherence interferometer*. Atmospheric aberrations are variable and degrade the contrast of long-exposure fringes, whereas optical aberrations are static and only change the average fringe phase. These interferometers superpose two wave-front with a relative rotation (Roddier & Roddier, 1973) or mirror flip (Dainty & Scaddan, 1975). The baseline r changes across the pupil, and so does the

contrast of long-exposure fringes $\gamma(r)$,

$$\gamma(r) = \exp[-3.44(r/r_0)^{5/3}]. \quad (1)$$

This method is theoretically perfect, but still affected by the guiding errors. Yet another problem is that Eq. 1 is accurate only for an infinite outer scale L_0. A realistic outer scale $L_0 \sim 20\,\mathrm{m}$ affects the coherence even at baselines of $r \sim 0.1\,\mathrm{m}$. The method still works, because we measure the true coherence (hence the true PSF), but the r_0 estimate derived from Eq. 1 will always be biased to larger values unless L_0 is known. The influence of the outer scale can be used to advantage: by measuring the long-exposure PSF (or coherence) at optical and infrared wavelengths simultaneously, we can derive the pair of parameters (r_0, L_0) (Tokovinin et al., 2007).

3.2 Absolute image motion

Absolute tilt of a wave-front over a circular telescope aperture (also called image motion or angle-of-arrival) is related to the seeing as

$$\sigma_\alpha^2 = K(\lambda/D)^2(D/r_0)^{5/3}, \quad (2)$$

where the coefficient $K = 0.340$ if the tilt is defined as an average wave-front gradient, and $K = 0.360$ if the Zernike tilt (best-fitting plane) is meant. The coefficient K is different for a centrally-obstructed or a non-circular aperture (Sasiela, 1994). The motion of an image in the focal plane of a small telescope thus leads to the estimate of the σ_α^2 and seeing, r_0.

Both Eq. 2 and Eq. 1 are valid only for the Kolmogorov turbulence model, $L_0 = \infty$. The measured tilts can be corrupted by the telescope shake. So, the absolute-tilt methods and long-exposure techniques are similar. The advantage of tilt vs. PSF is that the aperture diameter D can be smaller than r_0. The problem of telescope shake can be avoided by firmly fixing the telescope during data acquisition. Of course, the star moves in the field, but this linear trend can be fitted and subtracted, leaving pure atmospheric signal, or we can measure only in the direction perpendicular to the diurnal motion. The Polar Star is the source of choice for the northern hemisphere, as it moves so slowly. Polar star motion was recorded both photographically (Harlan & Walker, 1965) and photo-electrically (Babcock, 1963; Scheglov, 1980). In the southern hemisphere, the telescope has to track the star, so the measurements are usually done in the declination direction, as in the Carnegie seeing monitor (Persson et al., 1990).

The sensitivity of absolute image motion to L_0 is exploited in the Generalized Seeing Monitor (GSM) to measure this parameter (Ziad et al., 2000). The outer scale is deduced from the covariance of the image motion in 4 telescopes on individual mounts, with the idea that tracking errors (in the declination direction) are mutually independent and thus do not bias the covariances. As an additional precaution, parabolic trend is subtracted to model slow drifts. The r_0 parameter is measured independently by the differential motion (see below). The covariances are normalized by $r_0^{-5/3}$ to remove their dependence on seeing and fitted to the model depending only on L_0.

To the first approximation, the image motion is proportional to the phase difference at the aperture borders. Phase difference over a large baseline can be measured also by an interferometer. The influence of finite outer scale L_0 is even greater at large baselines, so

interferometric data can be used to measure it, as long as an independent estimate of r_0 is available. A comparison of the GSM with a long-baseline interferometer demonstrated a good agreement between these two approaches (Ziad et al., 2004). In fact, the GSM was compared to the speed of the fringe motion in the interferometer which, of course, is proportional to the product of the wave-front tilt and the wind speed. It comes as no surprise that tilts measured by the interferometer and the GSM agree well.

3.3 Differential image motion

In a DIMM, the seeing is inferred from the variance of the differential wave-front tilts in two (or more) small apertures. Typically, circular apertures of diameter D with centers separated by a baseline B are used. The variance of the differential tilt is described by Eq. 2, but the coefficient K now depends on the B/D ratio, on the measurement direction (longitudinal is parallel to the baseline, transverse is perpendicular), and on the details of centroid calculation (Tokovinin, 2002b). Moreover, the DIMM response is affected by the optical propagation (neglected in the standard DIMM theory) and by optical aberrations (Tokovinin & Kornilov, 2007). So, a blind application of Eq. 2 would not give an accurate r_0 estimate unless additional care is taken to remove instrumental biases.

A DIMM can be considered as a simplest Shack-Hartmann *wave-front sensor* (WFS) with two sub-apertures. To the first approximation, differential tilts are related to the defocus and astigmatism aberrations over a full telescope aperture, i.e. the wave-front curvature. A WFS with more than two sub-apertures can measure these and higher-order aberrations. Any *adaptive-optics* (AO) system with such a sensor can be used to deduce the seeing. Indeed, most AO systems have a seeing estimator incorporated in their software (e.g. Fusco et al., 2004; Schöck et al., 2003). The advantage of this solution is that the seeing is measured on the optical path that is relevant for the AO itself, avoiding any assumptions about turbulence spatial distribution or stationarity.

To be fair, estimating the seeing and other atmospheric parameters from the AO loop data is not a simple matter. The response of a WFS is often non-linear and poorly calibrated. This does not matter much for the AO itself, as the WFS measures only residual aberrations of the compensated wave-front. In a closed loop, the atmospheric distortions are derived from the shape of the *deformable mirror* (DM), which, in turn, is deduced from the control signals (voltages) and from the more-or-less accurately known properties of each particular DM. The temporal response of the closed-loop AO must be taken into consideration, noise variance must be subtracted, etc. Accurate seeing measurement is never a high priority for any given AO project, so atmospheric parameters currently measured by AO systems should be taken with a grain of salt until detailed analysis of biases and inter-comparisons with other methods are done.

Using a single star, we can only measure integrated turbulence properties along the line of sight. With a double source, it is possible to separate different atmospheric layers using the principle of *crossed beams* (Fig. 2). This idea is so universal that it is found in various ROTSs and is also used on horizontal paths with crossed laser beams. In the region of the beam overlap, turbulence gives correlated signals, while on the remaining part of the path the signals are un-correlated. Simple geometry tells us that the sensed zone is at a distance $z = B/\theta$ from the receiver, where B is the distance between the beams at the receiver and θ is the small angle between the beams. We can measure the turbulence profile on the whole path by changing B, θ, or both. The resolution along the

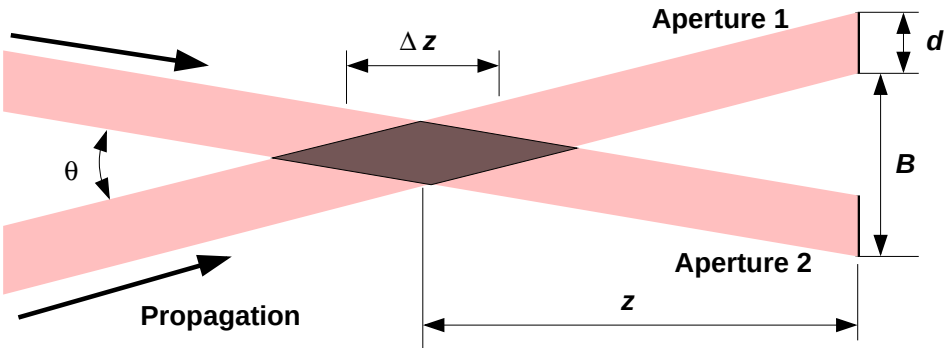

Figure 2: Principle of a crossed-beam ROTS. Two beams propagate from left to right toward receiving apertures. The dark area shows the beam overlap zone.

line-of-sight will be $\Delta z = d/\theta$, where d is the beam diameter.

One popular incarnation of the crossed-beam principle is SLODAR (SLOpe Detection And RAnging) (Wilson, 2002). It uses the double star with a fixed angular distance θ between the components as a light source. The wave-fronts are measured separately on each star using a standard WFS, usually (but not necessarily) of a Shack-Hartmann type. The number of resolution elements along the path equals the number of sub-apertures d across telescope diameter D, $N = D/d$. The sensing range extends from the telescope aperture to $z = D/\theta$ and depends on the separation θ of the chosen double star. The resolution is $\Delta z = z/N = d/\theta$. In a SLODAR, the average tilt over all apertures is subtracted and only the differential tilts are correlated. This makes the method immune to the telescope shake, but complicates data interpretation. To get a turbulence profile, the measured correlation between differential tilts of two stars is de-convolved with either theoretical or experimental tilt auto-correlation function as a kernel (Butterley et al., 2006).

Although SLODAR uses a standard WFS, it is a separate instrument, not part of an AO system. Care is taken to calibrate the WFS properly and to ensure un-biased slope measurements, marking a difference with current AO systems. Slope is easy to measure for sub-apertures of ~ 20 cm or larger because suitably bright double stars can be found, while the exposure time can be shorter than the sub-aperture crossing time d/V. However, it was possible to build a portable SLODAR with 5-cm sub-apertures by using a state-of-the art CCD detector with internal gain. This instrument has $N = 8$ sub-apertures on a 40-cm telescope.

The potential of the SLODAR method is not yet fully explored. It can measure a low-resolution turbulence profile in the whole atmosphere with a narrow double star or, alternatively, can use a very wide stellar pair for detailed, high-resolution profiling of the ground-layer turbulence. It is possible to extend the method to three or more stars. Multiple guide stars are necessary anyway for turbulence tomography in AO, so the signals from multiple WFSs will be available for SLODAR turbulence profiling (see also Tokovinin & Viard, 2001, for an alternative profiling method)

Another variation on the crossed-beam theme is a group of ROTSs where the baseline B is fixed and a multitude of sources with different angles θ is observed. The edge of the solar or lunar disks is such a convenient multi-θ source. Differential motion of the solar

limb is a standard method of daytime seeing measurement for solar astronomy (Beckers, 2001), although a DIMM can work in daytime with bright stars, too. The Moon is bright enough for night-time measurements. Recently, an experiment to measure differential tilts of the lunar limb, called MOSP (Moon Outer Scale Profiler), has been performed (Maire et al., 2007). So far, MOSP used only one full aperture. Differential tilt along the limb was measured and modeled. These tilts are sensitive to the turbulence outer scale L_0, so MOSP can, in principle, estimate the vertical profile $L_0(z)$. In the current implementation, an independent measurement of $C_n^2(z)$ is needed to model the data, but MOSP with two or more sub-apertures will be a self-sufficient ROTS that will measure both $C_n^2(z)$ and $L_0(z)$.

3.4 Scintillation

Twinkling of stars, *scintillation*, is caused by the optical turbulence and therefore can serve to characterize it. It is easier to measure flux than to measure wave-front tilts or phases. The optical propagation itself converts phase fluctuations to intensity variations, replacing "Instrument" in the general ROTS scheme (Fig. 1). All we need is just a detector!

The scintillation strength is characterized by the *scintillation index* σ_I^2,

$$\sigma_I^2 = \langle \Delta I^2 \rangle / \langle I \rangle^2, \tag{3}$$

where I is the instantaneous light intensity. Theory operates with the intensity distribution $I(x, y)$, in practice I is always averaged by some finite receiving aperture d or detector pixels.

The scintillation (speckle) pattern $I(x, y)$ (also called *flying shadows*) has a characteristic scale of the Fresnel radius $r_F = \sqrt{\lambda z}$, z being the propagation distance. Details larger than r_F can be described by geometric optics, as result of random focusing. Hence, for large apertures $d \gg r_F$, $\sigma_I^2 \propto z^2$. On the other hand, $\sigma_I^2 \propto z^{5/6}$ for the intensity fluctuations at a given point, or for small apertures $d \ll r_F$ (Roddier, 1981). Strong dependence of scintillation on z prevents us from interpreting scintillation index in terms of seeing unless the distance z is known. This means that a scintillation-based ROTS should measure somehow the turbulence profile (TP) $C_n^2(z)$. Yet another complication is the approximation of weak turbulence $\sigma_I^2 << 1$ used always in the data analysis but not always valid in the real life.

The first such instrument, Scintillation Detection and Ranging (SCIDAR), is based on the crossed-beams idea (Rocca et al., 1974; Vernin & Azouit, 1983). A binary star with angular separation θ produces the scintillation pattern where each detail is duplicated with a spatial shift θz. Of course, contributions from different layers are all mixed, but they can be recovered with correlation analysis, by computing the *covariance function* (CF)

$$C_I(\zeta, \eta) = \langle \Delta I(x + \zeta, y + \eta)\ \Delta I(x, y) \rangle\ /\ \langle I \rangle^2. \tag{4}$$

If the scintillation patterns from two stars were detected separately and cross-correlated, each turbulent layer would produce one peak shifted by θz from the coordinate origin. In a SCIDAR, the light of the stars is mixed together, so each layer produces a peak at the coordinate origin (self-correlation of each star) and a pair of symmetric peaks at $\pm\theta z$ (cross-correlation). The observed function $C_I(\zeta, \eta)$ is a superposition of all such triplets.

The profile can be extracted by de-convolving it with the known response function. It is relatively easy to identify and measure peaks produced by strong turbulent layers, but full deconvolution also recovers a smooth component of the TP which is not so obvious but can dominate the overall seeing.

As the width of the CF peak is of the order of r_F, the vertical resolution of SCIDAR is $\Delta z/z = \sqrt{\lambda z}/\theta z$. With a $10''$ binary and $z = 10\,\mathrm{km}$, SCIDAR has a vertical resolution $\Delta z \approx 1.5\,\mathrm{km}$. The size of the receiving aperture must be no less than θz, or 1 m if we want to reach 20 km with a $10''$ binary.

Turbulence near the telescope produces no scintillation. However, in a Generalized SCIDAR (G-SCIDAR) the detector is conjugated to the virtual plane below telescope aperture (Avila et al., 1997; Fuchs et al., 1998). This adds effectively some propagation path and permits to measure the complete TP. This virtual propagation is mathematically correct only when we neglect diffraction on the aperture border and optical aberrations, which is a reasonable approximation for telescopes above 1 m in size and conjugation planes some 2–5 km below the ground. Virtual propagation increases the scintillation index and associated departures from the weak-turbulence regime. All modern SCIDARS work in the generalized mode.

Apart from the TP, a SCIDAR can measure the wind speed in the atmosphere by correlating intensity patterns with some time lag τ. In such *spatio-temporal* correlation the peaks are displaced by $V\tau$. Again, it is easy to measure the speed of prominent peaks, but difficult to treat a general case of smoothly distributed turbulence. Automatic retrieval of both turbulence and wind profiles from G-SCIDAR data has been proposed and tested by Prieur et al. (2001).

If we select a very wide binary, the vertical resolution of a SCIDAR increases, at the expense of the altitude range. The idea of LOw-LAyer SCIDAR, LOLAS, is exactly this (Avila, 2007). Diffraction at the aperture edge becomes even more important, but its effect can be accounted for by modeling. LOLAS has been proposed for detailed profiling of the ground layer and used in the Mauna Kea Gemini campaign in 2007.

One practical disadvantage of both SCIDAR and LOLAS is a need of binary-star sources with suitable separations. As the choice of bright double stars on the sky is limited, these instruments must observe stars as faint as magnitude 5-7 for a quasi-continuous time coverage. Detectors of the highest possible sensitivity are required. The problem is more acute for LOLAS because its resolution element $\sqrt{\lambda z}$ is smaller. In fact, LOLAS uses an electron-multiplication CCD capable of detecting individual photons, like in the portable SLODAR.

It is frustrating to use faint double stars in a ROTS while so many bright single stars are available on the sky. Can a single star be somehow doubled? One suggestion was to observe the star at two different wavelengths, so that its image is doubled by the atmospheric dispersion, but this approach never worked in practice. On the other hand, temporal cross-correlation is a convenient way to get two identical but shifted patterns emulating a binary star. If the wind speed in the atmosphere is everywhere the same, $V(z) = \mathrm{const}$, the peaks produced by different layers still overlap in the CCF, but otherwise they are separated. This is the principle of the Single-Star SCIDAR (SSS), introduced by Caccia et al. (1987) and implemented recently (Habib et al., 2006). Recovering both wind and turbulence profiles from a set of correlation functions with different time lags τ is a very complex mathematical problem with possibly non-unique solution. It has been

demonstrated that SSS can detect and measure several strong layers in the atmosphere. It may be more difficult to recover a smooth $C_n^2(z)$ profile. The SSS has been proposed as a turbulence monitor working with a small aperture continuously. So far, it produced data only for short periods of time. The instrument itself is simple, but the data processing may be heavy.

A simpler approach to turbulence monitoring with a small telescope is implemented in the Multi-Aperture Scintillation Sensor, MASS (Kornilov et al., 2003; Tokovinin et al., 2003). Here we measure the scintillation of a single star through 4 concentric-ring apertures simultaneously. These apertures act as a spatial filter. The fluctuations of the intensity ratio between two such apertures, called *differential scintillation index*, do not have a steep dependence on z, as normal scintillations, but rather saturate for $\sqrt{\lambda z} > d$, where d is the average diameter of the apertures. This observable is directly related to the seeing produced by the high layers. Indeed, MASS gives very reliable measurements of the free-atmosphere seeing. On the other hand, its vertical resolution is only or the order $\Delta z/z = 2$, it is determined by the match between the Fresnel radius r_F and aperture diameters d_i. MASS uses the propagation theory to disentangle contributions of different altitudes by the size of the flying shadows. The idea is quite old (Peskoff, 1968), it was implemented in the scintillometer of Ochs et al. (1976). The success of MASS, compared to its predecessor, is explained by simultaneous 4-channel measurement and a careful treatment of instrumental effects and propagation. Small departures from the weak-scintillation theory are modeled and implemented in the data processing (Tokovinin & Kornilov, 2007). The atmospheric time constant τ_0 can be evaluated approximately by temporal analysis of scintillation in the smallest MASS aperture (Tokovinin, 2002a). MASS is usually combined with DIMM in a single instrument (Kornilov et al., 2007).

MASS does not sense turbulence near the ground. In principle, we can conjugate its apertures to a virtual plane below the telescope, like in a G-SCIDAR. The generalized MASS was tested and found to be impractical for several reasons. One fundamental consideration is that the scintillation produced by the near-ground turbulence in this regime is of fine spatial scale and small amplitude, i.e. difficult to measure. Using some other optical effect like tilt is a better choice. A comparison between LOLAS and SLODAR, two instruments for measuring the ground layer with scintillation and tilts, respectively, shows that the second method should be more sensitive.

Scintillation of extended sources such as planets or Moon is not seen by a naked eye; its amplitude is very small, but still not quite zero. A source of angular diameter θ averages flying shadows over a circle of diameter θz, acting in the same way as a receiving aperture. The combined effect of such averaging with propagation results in the *decrease* of scintillation with distance as $z^{-1/3}$, so that the maximum contribution comes now from very low altitudes $z \sim d/\theta$. With a receiver of $d = 1\,\mathrm{cm}$ diameter and the Sun ($\theta = 0.5°$), the maximum response is reached at $z \sim 1\,\mathrm{m}$.

The SHABAR instrument uses solar scintillation for measuring near-ground turbulence (Beckers, 2001). Six small photo-detectors are arranged in a linear non-redundant configuration with baselines up to 0.4 m. Pair-wise covariances of these signals give $n(n-1)/2 = 15$ numbers ($n = 6$) and permit to reconstruct the TP over the first 100 m above the observatory. SHABAR was one of the major components in selecting the site for the new solar telescope (Socas-Navarro et al., 2005). This site was not the best in terms of the measured seeing, but it has been proven with SHABAR that the seeing at

the height of the telescope tower will be superior over other sites.

A need to make similar assessment for night-time sites (i.e. to translate the seeing measured by a monitor to the level of the telescope) attracted attention to the lunar scintillometers. One such instrument has been constructed by Hickson & Lanzetta (2004), a 12-channel version is actually deployed at Cerro Tololo. Typical scintillation amplitude is small, $\Delta I/I \sim 10^{-4}$ ($\sigma_I^2 \sim 10^{-8}$), but the Moon is still bright enough to measure such signal reliably. Lunar phases complicate the data reduction but otherwise are not a major problem. Even a simplified 4-channel LUnar SCIntillometer, Lusci, can reliably measure the ground-layer seeing and differentiate contributions from several zones within the first 200 m above ground (Tokovinin et al., 2007).

The beauty of lunar and solar scintillometers is in their simplicity and robustness. With an extended source, the effective size of the averaging area (the largest of θz or d) is always larger than the Fresnel radius. Hence, the scintillation is determined by pure geometric optics, it is achromatic and immune to saturation. One caveat is that the the averaging scale θz exceeds 10 m for $z > 1$ km, hence the unknown outer scale L_0 changes drastically the high-altitude response of a scintillometer. This effect was found empirically in SHABAR and called "missing scintillation" (Socas-Navarro et al., 2005). Fortunately, it does not influence the response at low altitudes.

Scintillometers for turbulence measurements on a horizontal path are produced commercially by *Scintech*. By using large emitting and receiving apertures, these instruments work in the same geometric-optics regime as SHABAR, hence they are immune to the saturation and the turbulence inner scale. These effects would become significant if a narrow laser beam were used instead. Applications of scintillometers for measuring local turbulence (e.g. inside domes) can be envisioned, although high sensitivity is reached only on long propagation paths.

4 Future directions

4.1 New ROTS instruments

The inventory of existing ROTS methods shows a large variety of solutions and deliverables. Table 1 is not intended as a "shopping list" for a potential user, rather as an indication that many approaches are possible, and many more will come in the future. The most complete information on turbulence is provided by SCIDAR, albeit at a cost of large telescope aperture, high data flux and computer-intensive data processing. Simpler and cheaper instruments like DIMM or MASS are better suited for continuous turbulence monitoring. Each of the existing instruments can (and must) be improved in terms of data quality, but also simplicity, cost, and ease of operation. For example, it is found only recently that a DIMM is very sensitive to optical aberrations (Tokovinin & Kornilov, 2007).

It it unlikely that the explosive development of ROTS stops now. The progress of technology will continue to influence the implementation of the existing methods. Equally unlikely is the prospect that all basic methods are already known and will only be improved in the future. On the contrary, the number of ways in which information on turbulence can be extracted from the optical waves is unlimited. The field of ROTS (and optical propagation in general) is still young, so new methods and ideas will appear inevitably.

Table 1: Comparison between existing ROTS methods

Method	$C_n^2(z)$	$\mathbf{V}(z)$	r_0	θ_0	τ_0	L_0	Notes
Long-exposure PSF	-	-	+	-	-	+?	shake-sensitive
Coherence interferometer	-	-	+	-	-	-	shake-sensitive
Absolute tilts	-	-	+	-	-	+	shake-sensitive
DIMM or WFS	-	-	+	+?	-	-	standard method
GSM	-	-	+	+	+?	+	
SLODAR	+	+	+	+?	+?	-	double star
MOSP	+?	-	+?	+?	-	+	$L_0(z)$
SCIDAR	+	+	+	+	+	-	double star
LOLAS	+	-	-	-	-	-	GL only, double star
MASS	+	-	+?	+	+	-	low resol., FA
Single-Star SCIDAR	+	+	+	+	+	-	More tests needed
SHABAR	+	-	-	-	-	-	Sun or Moon, GL only
FADE	-	-	+	-	+	-	New instrument

One example of a new approach is the FAst DEfocus monitor, FADE (Kellerer & Tokovinin, 2007; Tokovinin et al., 2007). It is a descendant of DIMM where two apertures are replaced by a continuous ring. The radius of the ring-like image formed in the focal plane changes due to the atmospheric defocus aberration, so that seeing can be deduced from these fluctuations. Unlike DIMM, FADE is circularly symmetric, therefore temporal characteristics of the focus fluctuations do not depend on the wind direction. It has been shown that the speed of the focus variation is directly related to the atmospheric time constant τ_0, and, in fact, FADE has been developed explicitly for measuring this parameter.

The birth of FADE illustrates several aspects of future ROTSs. First, the instrument answers a practical need to monitor τ_0 with a small telescope (specifically related to the Antarctic site-testing program). Second, it was enabled by the new technology, fast image acquisition with a machine-vision CCD camera. Finally, the interpretation of the signal in terms of τ_0 required some analytical development and numerical simulations. Conceivably, these three ingredients – *practical need, new technology, and advanced theory* – will be present in all future ROTSs as well.

One potentially fruitful approach will be to capture and analyze defocused stellar images in a small (20–30 cm) telescope. Technically, this is simpler than MASS and DIMM, but can potentially provide similar information on turbulence. An ingredient still missing here is an adequate theory.

4.2 Sensitivity limit

Is there a fundamental limit to the sensitivity of a ROTS? Only a very general argument can be given here. Let the spatial size of the measured optical perturbations (aperture, detector pixel, etc.) be d. The time resolution has to be of the order $\tau = d/V$, where V is the maximum wind speed. So, the number of photons in each instantaneous exposure $N \propto d^2\tau = d^3/V$. The relative variance of the flux caused by the photon noise is proportional to $1/N$. Turbulence-induced phase variance is proportional to $d^{5/3}$ and produces some

fluctuations of the detected flux in a ROTS – its signal. So, generally speaking, the signal-to-noise ratio should be proportional to $d^{11/3}/V$. The sensitivity is a very strong function of the aperture (spatial resolution) of a ROTS, hence small apertures are restricted to bright light sources.

State-of-the art detectors with single-photon detection permit to make a smaller ROTS, up to a certain limit. For example, a SLODAR with 40-cm aperture cannot be made even smaller, as its limit is already reached. A typical DIMM uses baseline of 20 cm or more because its sensitivity with a smaller telescope would not be adequate. A MASS with 1-cm inner aperture could measure turbulence at 200 m altitude, but only with stars of magnitude zero. Even with current 2-cm inner aperture, the differential scintillation signal in a MASS is often smaller than the photon noise which is, of course, subtracted from the measured variance.

We conclude that many existing ROTSs are already close to their respective sensitivity limits. However, there is no universal limit. Even weak turbulence can be measured with a faint source by using an adequately large aperture and/or by designing an instrument that translates small perturbations to large flux variations. For example a 15-th magnitude star used for guiding and astigmatism correction in a 2x2 Shack-Hartmann sensor on a 8-m telescope is probably bright enough to measure the seeing.

4.3 Practical recommendations

Practical difficulties encountered in the implementation of ROTSa are not obvious from the general principles outlined above. Here are some comments to illustrate the point.

Existing seeing monitors use different components and software and often require substantial efforts in maintenance and data quality control. The "cost of ownership" may be quite high. An observatory wishing to install or improve a seeing monitor discovers that there are no trusted commercial suppliers of such instruments. Eventually they copy or buy an instrument from some other observatory. The *need for standard, commercially available ROTSs* is evident. Hopefully, the reduced cost of detectors and computers will help in fulfilling this need. Site-testing equipment procured commercially in the recent years by large-telescope programs is still too expensive. A future site monitor must be a "set-and-forget" thing at accessible price, like a standard meteo-equipment.

It turns out that the key missing component is not a ROTS itself but its feeding telescope. Amateur robotic telescopes are cheap and unreliable, professional telescopes are expensive and... also unreliable. Most problems in the operation of a ROTS are usually telescope-related. Development of a common *robotic telescope platform* is much needed to facilitate the implementation of ROTSs.

The data products of a ROTS are turbulence parameters in well-defined physical units, e.g. seeing in arc-seconds or turbulence integral in $m^{1/3}$. Each method can, in principle, provide such data by relying on its principle, theory, and internal calibrations. External calibration or "validation" is not needed. Of course, it is a good metrology practice to inter-compare the instruments. Inter-comparisons help to detect and eventually eliminate various instrumental biases. An old tradition of *inter-calibrating* seeing monitors, i.e. establishing empirical corrections to bring the data onto a "common system" should be abandoned once and for all. If an instrument produces biased data, empirical corrections do not help because the bias depends on the atmospheric conditions. Two instruments

can agree perfectly at one site or on one night (e.g. with slow wind speed) and diverge under different circumstances.

Turbulence measurements differ from most other measurements in one significant aspect: they cannot be repeated. This places a requirement for strict control of the data quality and biases *at the moment of acquisition*. Data quality is a new concept in the field of ROTS; most existing instruments either do not implement it or have only partial quality checks. This will change progressively in the future.

A need for a ROTS is not always justified. Adaptive optics, a major user of turbulence data, can deduce all required turbulence parameters from the AO instrument itself. Such information would be more relevant than the "site data" from a stand-alone ROTS. Development of reliable on-line extraction of atmospheric parameters from the AO loop data is still much needed. Similarly, estimates of the seeing obtained through the telescope are to be preferred over site-monitor seeing for queue-scheduled observatory operation or *a posteriori* data analysis. Modern telescopes equipped with fast guiders and active optics have all hardware functionality for on-line seeing measurements, but never use it.

References

Avila, R., Vernin, J., Masciadri, E., 1997, Appl. Opt., 36, 7898

Avila, R., 2007, Low Layer SCIDAR: a turbulence profiler for the first kilometer with very high altitude-resolution. Symposium on Seeing, Kona, March 2007.

Babcock, H.W., 1963, PASP, 65, 229

Beckers, J., 2001, Exp. Astr., 12, 1

Butterley, T., Wilson, R.W., & Sarazin, M., 2006, MNRAS, 369, 835

Caccia, J.L., Azouit, M., & Vernin, J., 1987, Appl. Opt., 26, 1288

Chernov, L.A., 1960, Wave Propagation in Random Media. Dover, New York.

Coulman, C.E., 1985, Ann. Rev. Astr. Astroph., 23, 19

Dainty, J.C. & Scaddan, R.J., 1975, MNRAS, 170, 519

Fuchs, A., Tallon, M., & Vernin, J., 1998, PASP, 110, 86

Fusco, T., Rousset, G., Rabaud, D. et al. 2004, J. Opt. (Paris), 6, 585

Gillingham, P.R., 1978, AAT Dome Seeing, a Progress Report. Anglo-Australian Observatory, Epping.

Habib, A., Vernin, J., Benkhaldoun, Z., & Lanteri, H., 2006, MNRAS, 368, 1456

Harlan, E.A. & Walker, M.F., 1965, PASP, 77, 246

Hickson, P. & Lanzetta, K., 2004, PASP, 116, 1143

Hosefeld, R., 1954, JOSA, 44, 284

Kellerer, A. & Tokovinin, A., 2007, A&A, 461, 775

Kornilov, V., Tokovinin, A., Voziakova, O., Zaitsev, A., Shatsky, N., Potanin, S., Sarazin, M., 2003, Proc. SPIE, 4839, 837

Kornilov, V., Tokovinin, A., Shatsky, N., Voziakova, O., Potatin, S., & Safonov, B., 2007, MNRAS, 383, 1268

Maire, J., Ziad, A., Borgnino, J. & Martin, F., 2007, MNRAS, 377, 1236

Ochs, G.R., Wang, T., Lawrence, R.S., & Clifford, S.F., 1976, Appl. Opt., 15, 2504

Persson, S.E., Carr, D.M., & Jackobs, J., 1990, Exp. Astr., 1, 195 [This is wrong Ref!]

Peskoff, A., 1968, JOSA, 58, 1032

Prieur, J.-L., Daigne, G., & Avila, R., 2001, Astron. Astroph., 371, 366

Rocca, A., Roddier, F., & Vernin, J., 1974, JOSA, 64, 1000

Roddier, C. & Roddier, F., 1973, JOSA, 63, 661

Roddier, F. 1981, Progress in Optics, 19, 281

Sarazin, M., & Roddier, F. 1990, Astron. & Astrophys., 227, 294

Sasiela, R.J., 1994, Electromagnetic wave Propagation in Turbulence. Springer-Verlag, Berlin.

Schöck, M., Le Mignant, D., Chanan, G.A., & Wizinowich, P.L., 2003, Proc. SPIE, 4839, 813

Sheglov, P.V., 1980, Astron. Tsirk., 1124, 3 (in Rusian)

Socas-Navarro, H., Beckers, J., Brandt, P. et al., 2005, PASP, 117, 1296

Stock, J. & Keller, G., 1961, in: Stars and Stellar Sysytems, eds. Kuiper, G.P. & Middlehurst, B.M., Chicago Univ. Press, Chicago, V. 1. p. 138.

Tatarskii, V.I., 1961, Wave Propagation in a Turbulent Medium. Dover, New York.

Tokovinin, A. & Viard, E., 2001, JOSA, 18, 873

Tokovinin, A., Kornilov, V., Shatsky, N., Voziakova, O., 2003, MNRAS, 2003, 343, 891

Tokovinin, A., 2002a, Appl. Opt., 41, 957

Tokovinin, A., 2002b, PASP, 114, 1156

Tokovinin, A., Sarazin, M., & Smette, A., 2007, MNRAS, 378, 701

Tokovinin, A. & Kornilov, V., 2007, MNRAS, 381, 1179

Tokovinin, A., Rajagopal, J., Bustos, E., & Thomas-Osip, J., 2007, Characterizing ground-layer turbulence with a simple lunar scintillometer. Symposium on Seeing, Kona, March 2007.

Tokovinin A., Kellerer A., Coude Du Foresto V., 2007, A&A, in print

Vernin, J. & Azouit, M., 1983, J. Opt. (Paris), 14, 131

Wilson, R.W., 2002, MNRAS, 337, 103

Ziad, A., Conan, R., Tokovinin, A., Martin, F., & Borgnino, J., 2000, Appl. Opt., 39, 5415

Ziad, A., Schöck, M., Chanan, G., Troy, M., Dekany, R., Labe, B.F., Borgnino, J., & Martin, F., 2004, Appl. Opt., 43, 2316